Computational AeroAcoustics: from acoustic sources modeling to farfield radiated noise prediction

Verification of higher-order discontinuous Galerkin method for hexahedral elements

Hüseyin Özdemir *, Rob Hagmeijer, Hendrik Willem Marie Hoeijmakers

Department of Mechanical Engineering, University of Twente, P.O. Box 217, 7500 AE, Enschede, The Netherlands

Available online 8 September 2005

Abstract

A high-order implementation of the Discontinuous Galerkin (DG) method is presented for solving the three-dimensional Linearized Euler Equations on an unstructured hexahedral grid. The method is based on a quadrature free implementation and the high-order accuracy is obtained by employing higher-degree polynomials as basis functions. The present implementation is up to fourth-order accurate in space. For the time discretization a four-stage Runge–Kutta scheme is used which is fourth-order accurate. Non-reflecting boundary conditions are implemented at the boundaries of the computational domain. The method is verified for the case of the convection of a 1D compact acoustic disturbance. The numerical results show that the rate of convergence of the method is of order $p + 1$ in the mesh size, with p the order of the basis functions. This observation is in agreement with analysis presented in the literature. *To cite this article: H. Özdemir et al., C. R. Mecanique 333 (2005).*
© 2005 Académie des sciences. Published by Elsevier SAS. All rights reserved.

Résumé

Vérification d'une méthode de Galerkine discontinue d'ordre élevé pour des éléments hexaédriques. L'implantation d'une méthode de Galerkine discontinue d'ordre élevé est présentée pour résoudre les équations d'Euler linéarisées tridimen-sionnelles en maillage non structuré avec des éléments hexaédriques. La méthode est basée sur l'utilisation de formules de quadrature non définies à l'avance et l'ordre élevé de la méthode est obtenu en utilisant des polynômes de degré élevé comme fonctions de base. La technique implantée est précise jusqu'à l'ordre 4 en espace. Pour la discrétisation en temps une méthode de Runge–Kutta précise à l'ordre 4 est utilisé. Des conditions aux limites non réfléchissantes sont implantées aux frontières du domaine de calcul. La méthode est validée sur le cas 1D d'une perturbation acoustique. Les résultats numériques montrent que le taux de convergence de la méthode est d'ordre p, p étant l'ordre des fonctions de base. Ce résultat est en accord avec les analyses présentées dans la littérature. *Pour citer cet article : H. Özdemir et al., C. R. Mecanique 333 (2005).*
© 2005 Académie des sciences. Published by Elsevier SAS. All rights reserved.

Keywords: Acoustics; Computational aeroacoustics; Discontinuous Galerkin method; Finite element method; Hexahedral elements

Mots-clés : Acoustique ; Aéroacoustique numérique ; Méthode de Galerkine discontinue ; Méthode des éléments finis ; Éléments hexaédriques

* Corresponding author.
 E-mail addresses: h.ozdemir@ctw.utwente.nl (H. Özdemir), r.hagmeijer@ctw.utwente.nl (R. Hagmeijer),
h.w.m.hoeijmakers@ctw.utwente.nl (H.W.M. Hoeijmakers).

1. Introduction

Compared to computational fluid dynamics the accuracy of numerical methods for aeroacoustics require special attention in the sense that numerical dispersion and dissipation errors are much more critical. Although finite-difference methods could be used to achieve higher-order accuracy, they need special treatments at the boundaries and usually require smooth, structured meshes. Especially when the problem of interest involves complex geometries this requirement cannot be met. The Discontinuous Galerkin (DG) method [1,2] has some remarkable advantages with respect to flexibility in discretization of domains with complex geometries. The DG method is a highly compact finite-element projection method which provides a practical framework for the development of a higher-order method desired for computational aeroacoustics on non-smooth unstructured grids [3–5]. In recent studies it has been shown that the accuracy is of order larger than $p + 1/2$, while the spatial dispersion error is of order $2p + 3$ and the spatial dissipation error is of order $2p + 2$ [6]. The treatment of the boundary conditions is relatively simple (no special treatment required), and obtaining uniform high-order accuracy at the boundaries involving complex geometries is feasible. In the present paper a high-order implementation of the DG method is presented for solving the three-dimensional Linearized Euler Equations on an unstructured hexahedral grid. The method is based on a quadrature-free implementation and the high-order accuracy is obtained by employing higher-degree polynomials as basis functions.

2. Quadrature free discontinuous Galerkin method

We consider the following three-dimensional Linearized Euler Equations (LEE):

$$L(\mathbf{u}) = \frac{\partial \mathbf{u}}{\partial t} + \frac{\partial \mathbf{f}_i(\mathbf{u})}{\partial x_i} = \mathbf{s}, \quad \mathbf{x} \in \Omega, \ t \in I_t \tag{1}$$

with initial and boundary conditions and,

$$\mathbf{f}_i(\mathbf{u}) = A_i(\mathbf{u}_0)\mathbf{u}, \quad A_i \in \mathbb{R}^5 \times \mathbb{R}^5$$

$$A_i(\mathbf{u}_0) = \begin{bmatrix} u_{0i} & \delta_{i1}\rho_0 & \delta_{i2}\rho_0 & \delta_{i3}\rho_0 & 0 \\ 0 & u_{0i} & 0 & 0 & \delta_{1i}/\rho_0 \\ 0 & 0 & u_{0i} & 0 & \delta_{2i}/\rho_0 \\ 0 & 0 & 0 & u_{0i} & \delta_{3i}/\rho_0 \\ 0 & \delta_{i1}\gamma p_0 & \delta_{i2}\gamma p_0 & \delta_{i3}\gamma p_0 & u_{0i} \end{bmatrix}, \quad i = 1, 2, 3 \tag{2}$$

where $\mathbf{u}_0$ is the reference state vector, $\mathbf{s} \in \mathbb{R}^5$ is the source term, $\Omega \in \mathbb{R}^3$ is an open domain with boundary $\partial\Omega$ and $t \in I_t$ denotes time, where $I_t \in \mathbb{R}^+ \setminus \{0\}$. Furthermore, the matrices A_i, $i = 1, 2, 3$, are real and have real eigenvalues, i.e., the system is hyperbolic. At $t = 0$ initial conditions are applied. The solution vector $\mathbf{u} : \Omega \times I_t \mapsto \mathbb{R}^5$ is given by $\mathbf{u} = (\rho', u_1', u_2', u_3', p')^{\mathrm{T}}$, where the components of the vector denote the dimensionless perturbations of the primitive variables: density, velocities (three directions) and pressure, respectively. Note that the formulation presented above is not restricted to isentropic flows and entropy waves are allowed.

We discretize the Linearized Euler equations (LEE) (Eq. (1)) in space, employing the Discontinuous Galerkin (DG) method in a region Ω. We consider a solution $\mathbf{u}(\cdot, t)$ such that for each time $t \in I_t$, $\mathbf{u}(\cdot, t)$ belongs to the function space U of the form $\mathbf{u}(\cdot, t) \in U^5$, $U \equiv L^2(\Omega)$, where $L^2(\Omega)$ denotes a Hilbert space of all square integrable functions on Ω with an associated inner product $\langle \cdot, \cdot \rangle$. The weak formulation of the LEE can be written as

$$\langle L(\mathbf{u}(\cdot, t)), \mathbf{v} \rangle = \langle \mathbf{s}, \mathbf{v} \rangle, \quad \forall \mathbf{v} \in U^5 \tag{3}$$

In order to discretize the LEE we divide the solution domain Ω into non-overlapping hexahedral elements Ω_j such that $\overline{\Omega} = \bigcup_{j=1}^{N_e} \overline{\Omega}_j$, where $\overline{\Omega}_j = \Omega_j \cup \partial\Omega_j$ is the closure of Ω_j and the boundary $\partial\Omega_j$ belongs to at most two

elements and N_e denotes the number of elements. In the semi-discrete formulation we consider the approximation $\mathbf{u}_h(\cdot, t)$, of the solution $\mathbf{u}(\cdot, t)$ as an expansion onto the basis set $\{b_{jk}\}$

$$\mathbf{u}_h(\mathbf{x}, t) = \sum_{j=1}^{N_e} \mathbf{u}_{jk}(t) b_{jk}(\mathbf{x}) \tag{4}$$

with, $\mathbf{u}_{jk} \in L^2(I_t)$ and $b_{jk} \in L^2(\Omega)$. It is noted that we employ the Einstein summation convention, except for the index "j". The $\mathbf{u}_{jk}$ are the solution expansion coefficients of the solution on Ω_j and functions of time only. The functions $\{b_{jk}\}$ are linearly independent basis functions defined such that

$$b_{jk} \equiv \begin{cases} \bar{b}_{jk}(\mathbf{x}), & \mathbf{x} \notin \partial \Omega_j, \\ 0, & \mathbf{x} \in \partial \Omega_j, \end{cases} \quad \bar{b}_{jk}(\mathbf{x}) = 0, \ \mathbf{x} \notin \overline{\Omega}_j \tag{5}$$

The functions $\bar{b}_{jk}$ and b_{jk} differ only in that $b_{jk} = 0$ on the boundary $\partial \Omega_j$ while in general $\bar{b}_{jk} \neq 0$ on the boundary $\partial \Omega_j$. The basis functions are continuous in Ω_j and $k = 0, 1, \ldots, M$ is the index of the polynomials where the upper limit is defined as

$$M(p, d) = \frac{1}{d!} \prod_{l=1}^{d} (p + l) \tag{6}$$

with d the number of space dimensions and p the highest degree of the polynomials used. We approximate the weak formulation (Eq. (3)) by

$$\langle L(\mathbf{u}_h(\cdot, t)), b_{jm} \rangle = \langle \mathbf{s}, b_{jm} \rangle, \quad \forall j \in (1, 2, \ldots, N_e), \ \forall m \in (0, 1, \ldots, M) \tag{7}$$

Using Eqs. (1), upon partial integration and applying Gauss' theorem we evaluate Eq. (7) for every basis function b_{jm},

$$\int_{\Omega_j} \frac{\partial \mathbf{u}_{jk}}{\partial t} b_{jk} b_{jm} \, \mathrm{d}\Omega - \int_{\Omega_j} \mathbf{f}_{ji} \frac{\partial b_{jm}}{\partial x_i} \, \mathrm{d}\Omega + \int_{\partial \Omega_j} b_{jm} \mathbf{f}_{ji} n_{ji} \, \mathrm{d}S = \int_{\Omega_j} \mathbf{s} b_{jm} \, \mathrm{d}\Omega \tag{8}$$

where $\mathbf{f}_{ji} \equiv A_i \mathbf{u}_{jk} b_{jk}$. At any interface between two elements, since the solution is allowed to be discontinuous, there is a left state and a right state leading to a Riemann problem. Solving the Riemann problem will provide the coupling and handle the discontinuity at element interfaces. Various kinds of flux formulas have been proposed and used in the literature to approximate the Riemann problem. In this study we employ the *Lax–Friedrich* flux formula of the form

$$\mathbf{h}(\mathbf{u}^L, \mathbf{u}^R, \mathbf{n}) = \frac{1}{2} \{ \mathbf{f}(\mathbf{u}^L) + \mathbf{f}(\mathbf{u}^R) - \theta |a|_{\max}(\mathbf{u}^R - \mathbf{u}^L) \}, \quad \theta \geqslant 0 \tag{9}$$

where, $|a|_{\max}$ is the maximum (absolute value) of the eigenvalues of the (5×5) matrix A_i, $\mathbf{u}^L$ and $\mathbf{u}^R$ are the values of the $\mathbf{u}_{jk}$ at the interface calculated using expansion coefficients of the elements at the left and right of that interface.

The basis functions are defined on the 'master' or 'reference' element $\widehat{\Omega}$, in the computational space. The local coordinates in the master element are given by $\boldsymbol{\xi} = (\xi, \eta, \zeta)^{\mathrm{T}}$ and the coordinate system has its origin at the centroid of the hexahedron $\widehat{\Omega} \equiv (-1, 1)^3$. The physical coordinates in element Ω_j are related to the computational coordinates in $\widehat{\Omega}$ by a map $\mathbf{x}^j(\boldsymbol{\xi})$ and an inverse map $\boldsymbol{\xi}^j(\mathbf{x})$. Assuming that the physical elements are restricted to parallelepiped, both maps are linear, but for a constant. On $\overline{\widehat{\Omega}}$ we define a set of linearly independent polynomials $\{b_k(\xi, \eta, \zeta)\}$ of degree $\leqslant p$:

$$\{b_k\} = \{\xi^{k_1} \eta^{k_2} \zeta^{k_3} \mid 0 \leqslant k_1 + k_2 + k_3 \leqslant p, \ k_i \geqslant 0\} \tag{10}$$
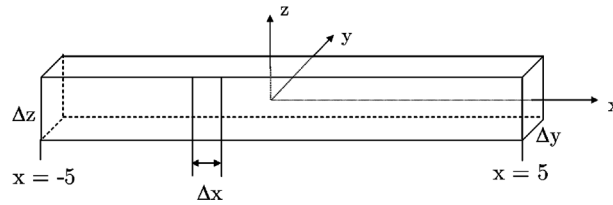
Fig. 1. The solution domain.

Fig. 1. Domaine de solution.

The compactness of the method results in an easy implementation of the boundary conditions. The boundary conditions can be implemented by prescribing the exact external solution ($\mathbf{u}_R$) or by reformulating the Lax–Friedrichs flux in terms of the interior solution ($\mathbf{u}_L$) and the physical boundary conditions. For the current implementation characteristic-based non-reflecting and symmetry-plane boundary conditions are used as described by Atkins [3].

The time integration is performed by a four-step, low storage Runge–Kutta algorithm [7] which is known to be fourth-order accurate for linear problems. Lesaint and Raviart [8] made the first analysis of the Discontinuous Galerkin method and proved a rate of convergence of at least h^p for general triangulations and of h^{p+1} for Cartesian grids employing basis polynomials up to order p, where h is a length scale that represents the size of elements. Later, Johnson and Pitkärata [1] proved a rate of convergence of at least $h^{p+1/2}$ for general triangulations and Peterson [9] numerically confirmed that this rate of convergence cannot be improved within the class of quasi-uniform meshes. Richter [10] obtained the optimal rate of convergence of h^{p+1} for a semi-uniform triangulation. Hence, when the method is applied to a hexahedral mesh, the analysis of Lesaint and Raviart indicates that the method is $(p + 1)$th-order accurate.

3. Convection of a 1D acoustic disturbance

As a test case Eqs. (1) are solved on a rectangular domain in which a compact 1D acoustic perturbation is imposed through the initial condition on the hexahedral grid. The solution domain has dimensions $x \in [-5, 5]$, while in the y–z plane it contains only one element, which is sufficient in order to represent the solution of the present 1D problem. However, note that the unknown coefficients $\mathbf{u}_{jk}$ associated with the basis functions that have a variation with respect to the y- and z-directions are not set to zero, but are computed as part of the solution. The initial acoustic perturbation is centered at $x = 0$. The simulations have been carried out with a quiescent background ($p_0 = 1$, $u_0 = 0$, $v_0 = 0$, $w_0 = 0$, $\rho_0 = 1$) without sources ($\mathbf{s} = 0$) and the initial 1D condition for the solution vector is given by:

$$\mathbf{u}(\mathbf{x}, 0) = \left(f(x), 0, 0, 0, f(x) \right)^{\mathrm{T}}, \quad f(x) = \mathrm{e}^{-\beta x^2}, \quad \beta = -\frac{\log(10^{-6})}{2} \tag{11}$$

3.1. Numerical results

The initial condition has been approximated by a Taylor-series expansion in each element which has the same spatial order of accuracy as the numerical method itself. The simulations have been performed with the present 3D method. Symmetry boundary conditions are used in y- and z-directions, while characteristic based non-reflecting boundary conditions are employed at the boundaries in x-direction. In the results presented below the disturbance remains small at the boundaries $x \pm 5$, i.e. the main part of the disturbance has not reached the boundary. The solution is presented along the line in x-direction passing through the centroid of the elements.
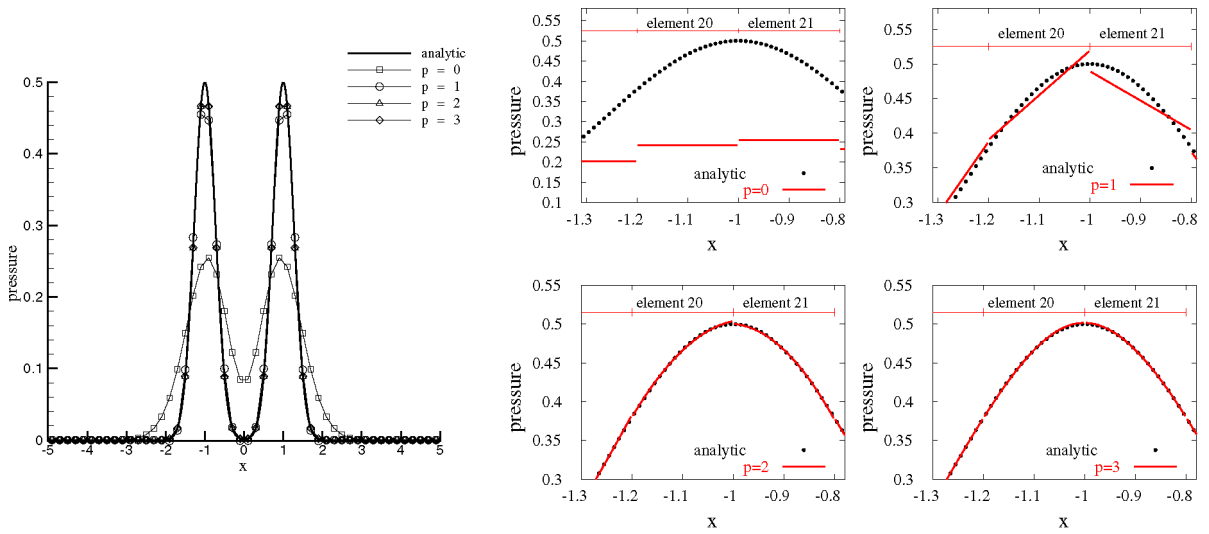
Fig. 2. Left: Distribution of pressure perturbation at dimensionless time $t = 1$ for $\Delta x = 0.2$, for the analytical and numerical solutions. The symbols indicate the numerical solutions, the solid line is the analytical result. Right: Reconstruction of the discontinuous solution at dimensionless time $t = 1$ and $\Delta x = 0.2$, for various values of p. The solid line indicate the discontinuous numerical solutions, the dotted line is the analytical result.

Fig. 2. A gauche : Distribution de la perturbation de pression au temps adimensionné $t = 1$ à $\Delta x = 0,2$, solution analytique et numérique. Les symboles représentent la solution numérique, le trait continu le résultat analytique. A droite : Reconstruction de la solution au temps adimensionné $t = 1$ à $\Delta x = 0,2$, pour différentes valeurs de p. Les traits représentent les solutions numériques discontinues, les traits pointillés le résultat analytique.

The simulations have been carried out on three different hexahedral meshes consisting of 100, 200 and 400 elements in x-direction, respectively. We obtained the time-converged solution by performing a time-refinement study. We can approximate the semi-discrete solution by employing Richardson extrapolation as follows:

$$\left| p'_{\Delta t} - p'_{\Delta t=0} \right| = c \Delta t^{\alpha} \tag{12}$$

where, $p'_{\Delta t}$ is the fully-discrete solution, $p'_{\Delta t=0}$ is the semi-discrete solution, c is a constant, Δt is the dimensionless time step and α is the order of accuracy of the time discretization. Performing simulations for different values of the dimensionless time step, Δt, we can construct the semi-discrete solution $p'_{\Delta t=0}$ for any point with the way explained above. Employing Eq. (12) at each grid point the order of accuracy of the time discretization, α, is obtained which is around 4. The time refinement study confirms that indeed the present implementation of four-stage low-storage Runge–Kutta scheme is fourth-order accurate in time for the linear problem considered.

The left-hand side of Fig. 2 shows a comparison of results for the first, second, third and fourth order accurate spatial discretizations, respectively, with the corresponding analytical solution for dimensionless time $t = 1$. The simulations have been performed on a relatively coarse mesh (number of elements in x-direction, $N = 50$) to clearly demonstrate the accuracy of the method when employing higher-order polynomials. The results show that for the first-order method the pressure perturbation dissipates quickly, while the higher-order methods give much better results. The right-hand side of Fig. 2 is the reconstruction of the discontinuous solution for various orders of accuracy. Here, the solution is evaluated at a large number (100) of points within each element, as a post processing, using the basis functions. When only an element-wise constant basis functions is used ($p = 0$) the solution can only be approximated element-wise constant. Increasing the polynomial degree to linear ($p = 1$) already gives a better approximation as can be seen from Fig. 2 qualitatively.
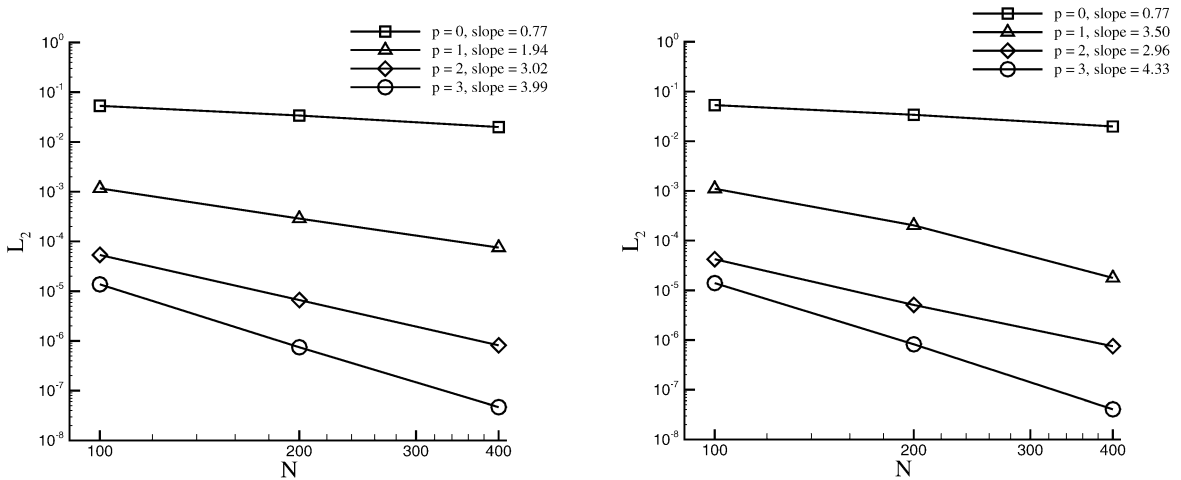
Fig. 3. Left: L_2-norm of error in pressure perturbation, Eq. (13) as function of N, with $\Delta x = L/N$, et $L = 10$, and $L = 10$, at dimensionless time $t = 1$. Right: The L_2-norm of error in pressure perturbation as function of N, with $\Delta x = L/N$, with $L = 10$, at dimensionless time $t = 1$ where fewer points are used to evaluate the L_2-norm.

Fig. 3. A gauche : Erreur en norme L_2 de la perturbation de pression, Eq. (13), en fonction de N, avec $\Delta x = L/N$, et $L = 10$, au temps adimensionné $t = 1$. A droite : Erreur en norme L_2 de la perturbation de pression, Eq. (13), en fonction de N, avec $\Delta x = L/N$, et $L = 10$, au temps adimensionné $t = 1$ où peu de points sont utilisés pour évaluer la norme L_2.

Next, a grid convergence study is performed using the time-converged semi-discrete solution. In order to perform this study, the solution is reconstructed on an interrogation mesh with 10 000 common points used for the meshes with 100, 200 and 400 elements in x-direction. The L_2-norm employed for each mesh, is of the form:

$$L_2 = \left\{ \frac{1}{L} \int_0^L \left[p'(x,t) - p'_{\text{exact}}(x,t) \right]^2 dx \right\}^{1/2} \cong \left\{ \frac{1}{10\,000} \sum_{j=1}^{10\,000} \left[p'(x_j,t) - p'_{\text{exact}}(x_j,t) \right]^2 \right\}^{1/2} \tag{13}$$

with x_j the points of the interrogation mesh, which gives an accurate approximation of the integral norm.

The left-hand side of Fig. 3 shows the L_2-norm of the error in the pressure perturbation as a function of the number of elements N, with $\Delta x = L/N$, and $L = 10$. The results show that the present method is converging at a rate of h^{p+1} for $p = 1, 2$ and 3 and with a rate slightly higher than $h^{p+1/2}$ for $p = 0$, which agrees with the convergence rates derived in the literature, e.g., [6]. It is remarkable that in the range of Δx considered the line of the order p method is situated above the one for the order-$(p - 1)$ method for any p considered.

It is also observed that in case fewer points are used to evaluate the L_2-norm, e.g., only the points of the coarsest grid, the rate of convergence for $p = 1$ is about h^3 (see the right-hand side of Fig. 3) which is one order higher than expected, which might suggest that this specific norm based on some special points in the solution, namely, points close to the intersection points.

4. Concluding remarks

A study has been carried out with respect to the verification of a method developed to solve the Linearized Euler Equations in three dimensions, employing a Discontinuous Galerkin spatial discretization on a hexahedral grid. Performing a time-refinement study it is confirmed that the method is fourth-order accurate in time employing a four-stage low-storage Runge–Kutta scheme. From the grid convergence study it is concluded that the method has a rate of convergence h^{p+1} for $p = 1, 2$ and 3 and slightly above $h^{p+1/2}$ for $p = 0$.

References

[1] C. Johnson, J. Pitkärata, An analysis of the discontinuous Galerkin method for a scalar hyperbolic equation, Math. Comput. 176 (1986) 1–26.

[2] B. Cockburn, S. Hou, C.W. Shu, TVB Runge–Kutta local projection discontinuous Galerkin finite element method for conservation laws II: General framework, Math. Comput. 186 (1989) 411–435.

[3] H.L. Atkins, Continued development of the discontinuous Galerkin method for computational aeroacoustic applications, AIAA paper 97-1581, 1997.

[4] C.P.A. Blom, R. Hagmeijer, E. Védy, Development of discontinuous Galerkin method for the linearized Euler equations, in: RTA/AVT Symposium on Development in Computational Aero- and Hydro-Acoustics, Manchester, UK, 2001.

[5] H. Özdemir, C.P.A. Blom, R. Hagmeijer, H.W.M. Hoeijmakers, Development of higher-order discontinuous Galerkin method on hexahedral elements, in: 10th AIAA/CEAS Aeroacoustics Conference, Manchester, 2004.

[6] F.Q. Hu, H.L. Atkins, Eigensolution analysis of discontinuous Galerkin method with non-uniform grids, Part I: One space dimension, J. Comput. Phys. 182 (2002) 516–545.

[7] A. Jameson, W. Schmidt, E. Turkel, Numerical solution of the Euler equations by finite volume methods using Runge–Kutta time-stepping schemes, AIAA paper 1981-1259, 1981.

[8] P. Lesaint, P.A. Raviart, On a finite element method for solving the neutron transport equation, in: Mathematical Aspects of Finite Elements in Partial Differential Equations, Academic Press, 1974.

[9] T. Peterson, A note on the convergence of the discontinuous Galerkin method for a scalar hyperbolic equation, SIAM J. Numer. Anal. 28 (1991) 133–140.

[10] G.R. Richter, An optimal-order error estimate for the discontinuous Galerkin method, Math. Comput. 50 (1988) 75–88.